Hindawi Publishing Corporation
Advances in Materials Science and Engineering
Volume 2016, Article ID 5954636, 10 pages
http://dx.doi.org/10.1155/2016/5954636

Research Article

Urea Formaldehyde Composites Reinforced with Sago Fibres Analysis by FTIR, TGA, and DSC

Tay Chen Chiang,[1] Sinin Hamdan,[1] and Mohd Shahril Osman[2]

[1]*Faculty of Engineering, Universiti Malaysia Sarawak, Jln Meranti, 94300 Kota Samarahan, Sarawak, Malaysia*
[2]*University College of Technology Sarawak, Persiaran Brooke, 96000 Sibu, Sarawak, Malaysia*

Correspondence should be addressed to Tay Chen Chiang; chenchiang@hotmail.my

Received 15 October 2015; Revised 1 December 2015; Accepted 7 December 2015

Academic Editor: Peter Majewski

Copyright © 2016 Tay Chen Chiang et al. This is an open access article distributed under the Creative Commons Attribution License, which permits unrestricted use, distribution, and reproduction in any medium, provided the original work is properly cited.

Agricultural material or biomaterial plays an important role in the field of fibre-reinforced polymeric materials with their new range of applications and achieves the ecological objective. Composition and structure of the nature fibre and matrix must be taken into consideration for the end use. In this project, Sago fibre particleboard bonds with Urea Formaldehyde to form composite. Fourier Transform Infrared (FTIR) spectra are used to characterize the Sago/Urea Formaldehyde composite in terms of their functional group and bonding. Sago/UF composite with smaller particle and higher loading of fibre with 15 wt% of UF matrix has the higher curing properties. The composite will have a denser structure by adopting bigger particle and higher loading of UF matrix. The Sago/UF composite only endures a single stage of decomposition. Thermal stability results indicate that particle size, particle/matrix interface adhesion, and particle loading have great influence on the thermal properties of the composites.

1. Introduction

Sago palm is the primary source of Sago. Sarawak, Malaysia, is a state that produces the most Sago plant and is the world's biggest exporter for Sago starch. The demand for Sago is increasing from year to year and the Sago pith waste increases after starch process. It is estimated that approximately 7 tons of Sago pith waste is produced daily from a single starch processing mill [1]. Improper disposal of Sago waste will cause negative impacts to the environment. To avoid this environmental issue, Sago waste is mixed with Urea Formaldehyde through hot pressing process to produce a particleboard. The production of particleboards involves large amount of binders (Urea Formaldehyde) which accounts for up to 32% of manufacturing cost in the glue-wood composite industry [2]. Hence, Sago/UF particleboards have become the new composite material in reducing the demand in the furniture industries.

In general, composite materials are used in the industry due to their attractive characteristics such as optimized performance, minimized weight and volume, and cost saving as well as chemical and biodegradation resistance [3].

The final properties of a composite are influenced by the properties of the fibre and the interfacial bonding of fibre and matrix [4]. The chemical bonding plays an important role in the bonding process between the matrix and fibre in a composite [4]. Researchers have reported that the critical particles size, particle-matrix interface adhesion, and particles loading on composite have notable effects on the mechanical properties [5]. Although natural fibres are frequently used as reinforcement, there are some drawbacks, such as poor compatibility with thermoplastic matrix, high moisture absorption, high probability of deterioration by biological organisms, and low thermal stability [6]. A thermal analysis was performed on the Sago particleboard to qualify the gravimetric response and specific heat capacity at elevated temperature. TGA was used to analyze the thermal stability of materials through decomposition stage as well as under a variety of conditions and examine the kinetics of physicochemical processes occurring in the sample [7]. Temperature also influences

the thermal stability of natural fibre composite. It causes thermal expansion or contraction and high hygroscopicity that lead to fibre swelling and deformation [8]. Moreover, DSC provides the quantitative and qualitative data on endothermic and exothermic process of materials during physical transitions that are caused by phase change, melting, glass transitions, thermodynamic process, kinetic events, crystallization, and oxidation.

To develop materials with lower environment impact, the solution proposed here is to associate Sago particles and UF matrix. The previous work was conducted to characterize the mechanical properties of particleboard made from Sago with different loading of UF matrix and particles size [9]. An understanding of adhesives and how they react to different particles size and weight fraction will help us understand the behaviour of Sago composite materials and design based on the desired function.

The objective of this project is to understand the thermal degradation behaviour of natural fibre/polymer composite subjected to thermal exposure and its constituents. Thermal sensitivities of various particle size and weight fraction are compared before it is applicable in the field.

2. Materials and Methods

2.1. Sago and Matrix Preparation. The particleboards were produced using Sago waste and Urea Formaldehyde as the matrix. Sago waste particles were collected from Mukah. The Sago waste went through the sieving process for size separation. Particles of less than 0.6 mm, 1.18 mm, and 2 mm sizes were selected and used in this experiment. After the sieving process, the particles were subjected to the drying process under the sun. The particles were dried in the oven with a temperature of 105°C for 24 hours to achieve moisture content of less than 5%. 51.5% of Urea Formaldehyde (UF) resin was obtained from Hexzachem Sarawak Sdn Bhd and served as a particle binder.

2.2. Particleboard Fabrication. Sago particles and Urea Formaldehyde (UF) were weighed to the desired weight and placed in the mixing drum for the mixing process. The core particles were mixed by spraying them with Urea Formaldehyde and hardener to achieve a homogeneous distribution of adhesives. After the blending process, the Sago particles were spread evenly into the 30 cm × 30 cm wooden mold using a stainless steel plate as base.

A thin layer of silicon glass mat was placed onto the caul plate to prevent the panel from being attached to the plate during hot press process. The mat was prepressed manually to consolidate the thickness. During hot press process, the distance bars were placed at both sides of the mat to obtain the desired thickness of the board. The mat then went through hot press process under the temperature of 160°C. The pressure of the hot press machine was set at 40 bar for 2 minutes and then gradually decreased to 20 bar and 10 bar for 2 minutes, respectively. After the hot press process, the boards were kept in the chamber with humidity of 65±5% and 25±2°C for 2-day curing process. The main purpose of curing is to stabilize the particleboards for constant evaluation.

Two categories of the samples are prepared for TGA, DSC, and FTIR:

(i) Sample prepared according to the particles size: sample A = 0.6 mm, sample B = 1.18 mm, and sample C = 2 mm with 15 wt% of UF matrix.

(ii) Sample prepared according to the weight fraction: sample D = 90 wt% Sago fibre + 10 wt% UF, sample E = 80 wt% Sago fibre + 20 wt% UF, and sample F = 70 wt% Sago fibre + 30 wt% UF.

2.3. Mechanical Test (Internal Bonding and Screw Test). Japanese Industrial Standard (JIS A 5908) for particleboards was used to evaluate the properties of the Sago particleboards [10]. Specimens with the dimension of 50 mm × 50 mm × 10 mm were prepared from each sample board for Internal Bonding and Screw Test. A screw with Ø 2.7 mm was driven into the center of specimen until the head of screw is parallel to the surface of the specimen. Specimens for Internal Bonding and Screw Test were tested by using the Instron machine (model 5566) with a loading speed of 2 mm/min.

2.4. Thermogravimetric Analysis (TGA) and Differential Scanning Calorimetry (DSC). The powder sample of particleboard was prepared. The thermal analysis of the sample was carried out using TGA/DSCI STAR System, Mettler Toledo thermal analyser according to ASTM E1131. Approximately 10 mg of the powder sample was placed in an aluminium pan and heated constantly at a rate of 10°C/min from 50°C to 800°C under 30 mL/min of nitrogen gas atmosphere. The weight loss and temperature were recorded and analysed to determine the following TGA parameters: weight loss %, initial degradation temperature, volatiles in sample, and the residual weight %. For DSC, the heat given off during a reaction was called an exotherm while the heat absorbed by material is called an endotherm. By measuring the exotherms and endotherms, it is possible to determine all the chemical and physical state changes that occurred in the sample.

2.5. Fourier Transform Infrared (FTIR). The functional groups and chemical characteristics of Sago/UF particleboards were obtained using a Fourier Transform Infrared Spectroscopy (Shimadzu, IRAFFINITY-1) with a resolution of 4000–600 cm^{-1} using 20 scans per sample.

3. Results and Discussion

3.1. Mechanical Properties of Sago Composite (Internal Bonding and Screw Test). Figures 1 and 2 show the effect of Sago particles size and weight fraction on the Internal Bonding and Screw Test. The result shows that sample B with particle size of 1.18 mm and sample E with 20 wt% of matrix have highest internal bonding strength. This is due to the fact that particle 1.18 mm has better bonding with the matrix in the particleboard where the particles and matrix had filled up the voids and increased the IB strength [11].

Sample C with coarse particles of 2 mm was not fully bonded with the matrix as there were voids around the Sago particles where the particle can pull out easily while fine

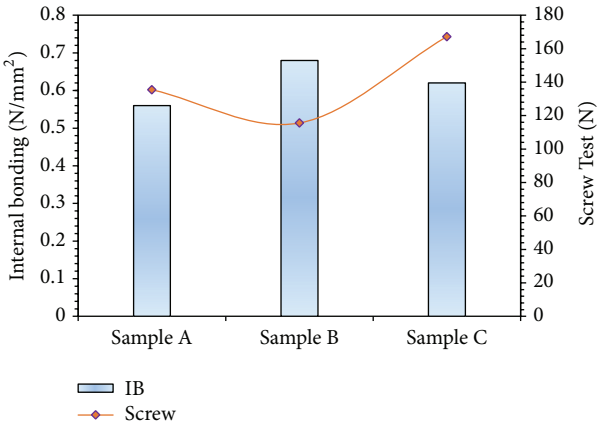

Figure 1: Effect of particles size on Internal Bonding and Screw Test.

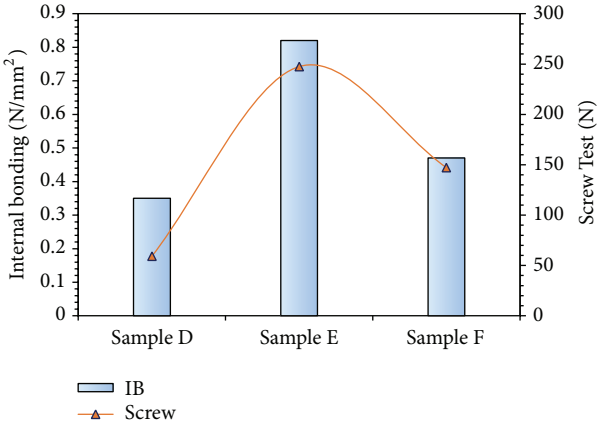

Figure 2: Effect of weight fraction on Internal Bonding and Screw Test.

particles of 0.6 mm in sample A have the lowest IB as it is difficult for excess matrix to flow smoothly between particles and were not fully penetrated into the Sago particles [12].

Sample E shows that the IB raises with an increase in UF by reaching a maximum weight fraction at 20 wt% as a result of the absence of voids in the particleboard creating good bonding between the particles and matrix [13, 14]. The result dropped after that due to the decrease of Sago particles which form the voids between each other and the excess matrix evaporated during the hot press process.

Besides, the internal bond strength of UF-bonded particleboards was largely depending on the strength of adhesive and its bonding to fibre and also depending on the degree of hydrogen bonding between molecules and condensation reactions between methylol and amide groups [15].

The Screw Test results are also displayed in Figures 1 and 2 where samples C and E had achieved the highest screw strength. The effective binding between the particles with matrix had increased the compatibility and enabled a screw to be fixed securely on the particleboard which resulted in better screw withdrawal reading [12, 16, 17]. Sample C with 2 mm sieving size of particles achieved the highest screw strength in view of the particles that possessed good structure in

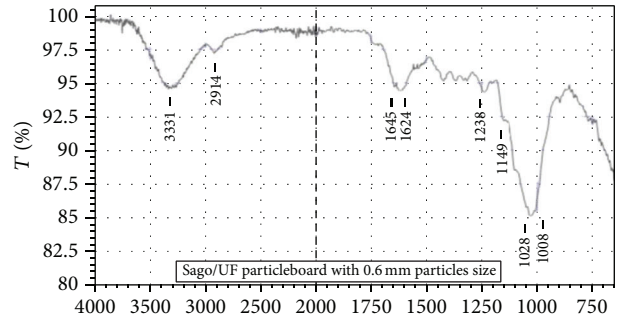

Figure 3: Sample A: Sago/UF Sample with particles size 0.6 mm.

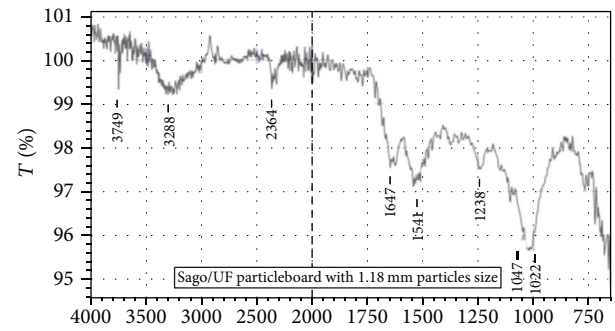

Figure 4: Sample B: Sago/UF Sample with particles size 1.18 mm.

the particleboard and the particles were sufficiently bonded by the matrix.

From the observation, sample E withdrawal strength improved at different levels as the resin content increased until certain limit of weight fraction. The higher the resin content, the higher the screw withdrawal load that it can endure [12, 13]. This is due to the ability of a board to bear the pulling force after being resinated with high resin dosage [18]. The boards with high resin caused the screw to be embedded tightly and resulted in better screw withdrawal strength. High compaction of a particleboard will increase the withdrawal strength as the particles were packed together with higher strength [18].

3.2. Characterization of Sago Composite with Different Particles Size. Similar pattern of FTIR spectra was observed in Figures 3, 4, and 5. The results show that a common absorption belongs to starch feature of natural material, which is polysaccharide in the region between 1200 and 1000 cm^{-1} [19].

FTIR spectra show the UF characteristics in a particleboard. The peak 2914 cm^{-1} represented C-H stretching of UF [19]. Both samples A and B have showed the similar chemical structure C=O stretching of primary amide at 1645 cm^{-1} and 1647 cm^{-1} [20]. The absorption bands of sample A at 1028 cm^{-1} and sample B at 1047 cm^{-1} were attributed to C-N or NCN stretching of methylene linkages (NCH_2N) [20]. The IR absorption band that corresponded to C-O group with stretching of aliphatic ether was observed at 1149 cm^{-1} [20].

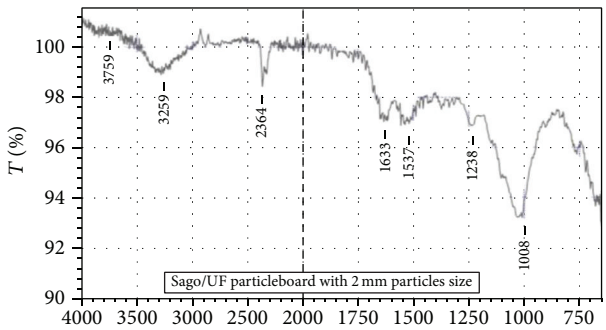

Figure 5: Sample C: Sago/UF Sample with particles size 2 mm.

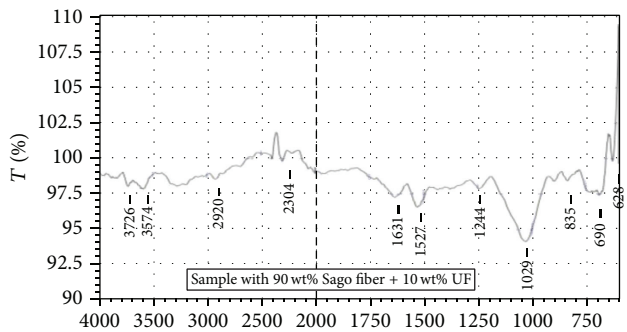

Figure 6: Sample D: Sago/UF Sample with 90 : 10.

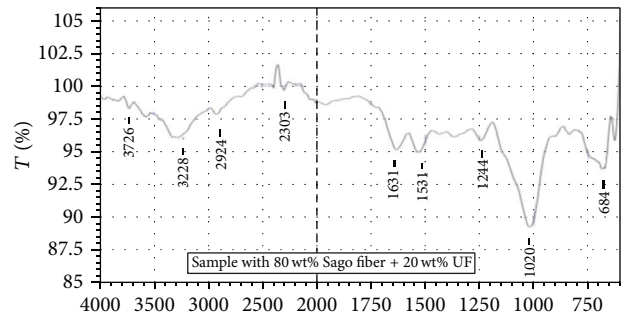

Figure 7: Sample E: Sago/UF Sample with 80 : 20.

The results show that sample B has better bonding compared to sample C due to the most occurring of chemical structure. All the Sago composites showed the N-H bending vibrations of UF at 1645 cm^{-1}, 1647 cm^{-1}, and 1633 cm^{-1}. This is due to the interaction between hydroxyl group with the amino group [21].

Sago fibre with absorption peak of 3900–3000 cm^{-1} showed starch characteristic. The presence of OH group at 3331 cm^{-1}, 3288 cm^{-1}, 3749 cm^{-1}, 3259 cm^{-1}, and 3759 cm^{-1} is related to the presence of amylose and amylopectin in Sago starch [22]. The peaks at 1624 cm^{-1}, 1645 cm^{-1}, and 1647 cm^{-1} were due to the tightly bound water molecules that were present in the Sago starch [22, 23]. The peak 1149 cm^{-1} was due to the OH group of starch that took part in the hydrogen bond formation [24]. C-O stretching in C-O-C and C-O-H in the glycosidic ring of Sago starch was observed at the range of 1100–990 cm^{-1} [23]. The absorption band at 1260–900 cm^{-1} was attributed to the stretching of C-O group. This change is caused by the rearrangement of hydrogen bonds between starch and fibre which implies the distinct interaction between the chains of polymers [22]. In Sago starch, the hydrogen bonded OH bond stretching vibration of α-cellulose was observed at 3331 cm^{-1}, 3288 cm^{-1}, 3749 cm^{-1}, 3259 cm^{-1}, and 3759 cm^{-1} [24]. The lower wavelengths were due to the fact that intermolecular hydrogen bonds in the glycosidic ring weaken the O-H bond. Hence, this has shifted the band absorption to lower frequency [23].

Sago fibres are associated with lignocellulosic components such as cellulose, hemicelluloses, and lignin. The cellulose is formed by glycosidic linkages and hydroxyl groups with small amount of carboxyl, whilst hemicellulose and lignin are dominated by ether bonds with carboxyl group. From Figures 3 and 4, the IR absorption band that corresponded to C-O, C=C, and C-C-O vibrational stretching was observed at 1028 cm^{-1} and 1022 cm^{-1}. 1149 cm^{-1} was attributed to C-O-C ring vibrational stretching of β glycosidic linkage for cellulose I and cellulose II. The peak at 1238 cm^{-1} showed the syringyl ring breathing and C-O stretching in lignin. On the other hand, 1624 cm^{-1}, 1647 cm^{-1}, and 1633 cm^{-1} corresponded to C=O stretching vibration in conjugated carbonyl of lignin and 2914 cm^{-1} belonged to C-H stretching of lignocellulosic components.

3.3. Characterization of Sago Composite with Different Weight Fraction. FTIR spectra in Figures 6, 7, and 8 show that samples D, E, and F were made from the same raw material. However, only samples D and E showed similar FTIR spectra pattern while sample F showed a significant different pattern. Several new absorption bands appeared in sample F. The IR absorption band corresponding to free hydroxyl group was observed at 3750 cm^{-1} due to the increase of UF and reduced Sago fibre. The wavebands were slightly different between each other as the bonding structure of starch inside the Sago particles and UF was different. The FTIR spectra showed a common feature of natural material, which is polysaccharide in the region 1200–1000 cm^{-1} [19].

Sago fibre has been attributed to some important characteristic of starch and was shown by the peak at 1629 cm^{-1} and 1631 cm^{-1} for N-H bending. The peak 1373 cm^{-1} appeared as C-H bending in methyl [19]. Peak 1260–900 cm^{-1} was attributed to the stretching of C-O group [23]. In fact, a slight increase in FTIR peak could be observed in sample F. Those changes could be interpreted in terms of the rearrangement of hydrogen bonds between Sago fibre and UF; hence, this indicated a distinct interaction between the chains of polymer [22].

Starch is characterized by two strong and broad absorption peaks occurring at 3900–3000 cm^{-1} and 1250–1000 cm^{-1} for O-H and C-O-C stretching, respectively [22]. The presence of OH group peaks at 3261 cm^{-1}, 3574 cm^{-1}, 3726 cm^{-1}, 3228 cm^{-1}, and 3726 cm^{-1} was related to the presence of amylose and amylopectin in Sago starch [22]. The characteristic peaks appeared due to the intermolecular hydrogen bond

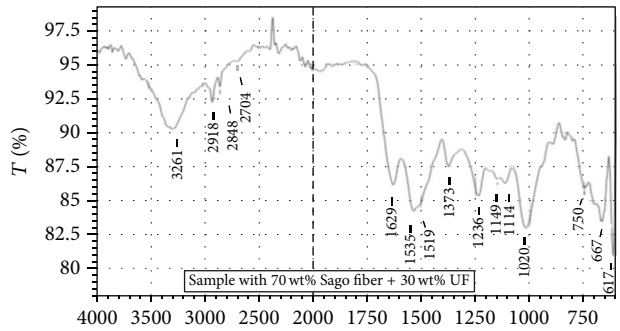

Figure 8: Sample F: Sago/UF Sample with 70 : 30.

formation that occurred when starch and UF were incorporated into the particleboard [22]. The peak which shifted from 1029 cm^{-1} to 1020 cm^{-1} showed that the glycerol is able to form a more stable hydrogen bond [25].

The absorption bands of sample F at 3261 cm^{-1} were due to O-H stretching vibration. Normally the absorption range for O-H vibration is 3700–3500 cm^{-1}, but the Sago starch has shifted to lower wavelength [23]. This is probably due to the intermolecular hydrogen bonds in the glycosidic ring that weaken the O-H bond and have shifted the absorption band region to lower frequency which is between 3400 and 3200 cm^{-1} [23]. The strong O-H stretching of sample D is at 3574 cm^{-1} and 3726 cm^{-1}, while the sample E is at 3228 cm^{-1} and 3726 cm^{-1} whereby the sample F only appeared once at 3261 cm^{-1}. Sample D showed higher wavelength in FTIR and this indicated the presence of higher volume of Sago particle in the particleboard compared with sample F. The absorption band at 2918 cm^{-1}, 2920 cm^{-1}, and 2924 cm^{-1} showed the C-H stretching [23]. Board with absorption range 1100–990 cm^{-1} was characterized by C-O stretching in C-O-C and C-O-H in the glycosidic ring of Sago starch [21]. Besides, weak bands that occurred in the range of 930–600 cm^{-1} were probably due to out-of-plane bonded O-H and C-H deformation [23].

The peaks positions at 1629 cm^{-1} and 1631 cm^{-1} were the weak absorption for Sago starch. This was probably due to the presence of tightly bound H_2O in the starch molecules [23, 25]. The peaks at 1629 cm^{-1} and 1631 cm^{-1} corresponded to N-H bending vibration. This indicated that the cellulose can be attributed to the interaction between hydroxyl groups and amino group [21].

The UF was successfully impregnated inside the particleboard as confirmed by FTIR spectroscopic analysis of particleboard. At sample F, the absorption with peaks 2704 cm^{-1}, 2848 cm^{-1}, and 2918 cm^{-1} showed the C-H stretching of lignocellulose component and aldehyde. The 3 peaks showed that high concentration of UF penetrated into the particleboard as compared to sample D with 2920 cm^{-1} and sample E with 2924 cm^{-1} with single peak only. The increased absorption band may be due to impregnation of UF inside the cell wall void spaces of Sago [26]. Observations of IR absorption band corresponding to free hydroxyl, N-H groups, and C-OH bond can be seen at 3750 cm^{-1}, 3574 cm^{-1}, and 3261 cm^{-1}. Such phenomenon could be attributed to hydrogen bonding between Sago and UF. This band became broader as UF increased, indicating an increase of hydrogen bonding. The IR absorption band that corresponded to CH group, C-O group, H–C=O, amide I, and amide II was observed at 2924 cm^{-1}, 1020 cm^{-1}, 2848 cm^{-1}, 1630 cm^{-1}, and 1530 cm^{-1}, respectively. As 30 wt% UF was added in sample F, two new peaks that corresponded to N-O were observed at 1519 cm^{-1} and 1373 cm^{-1}, and C-C-O group was observed at 1244 cm^{-1} but the peak shifted to 1236 cm^{-1}. UF showed those characteristics in sample F, 750 cm^{-1} assigned to C=O deformation of the NCON skeleton, 1149 cm^{-1} assigned to C-O stretching of aliphatic ether, and 1373 cm^{-1} that belongs to C-N stretching of CH_2-N [20]. Meanwhile, two new peaks that corresponded to C-O-C were observed at 1149 cm^{-1} and 1114 cm^{-1}, as 30 wt% UF was added. The C-H group was observed at 835 cm^{-1}, 690 cm^{-1}, and 628 cm^{-1}; as 30 wt% UF was added, these absorption peaks shifted to lower wavenumber, that is, 750 cm^{-1}, 667 cm^{-1}, and 617 cm^{-1}.

Based on the FTIR spectra, absorption bands at 2918 cm^{-1}, 2920 cm^{-1}, and 2924 cm^{-1} indicated C-H stretching of lignocellulosic components for organic matter [24]. The absorption bands are associated with the presence of lignocellulosic components as cellulose, hemicellulose, and lignin. The cellulose is formed by glycosidic linkages and hydroxyl group with a small amount of carboxyl, whilst hemicellulose and lignin are predominated by ether bonds with hemicellulose characterized by the amount of carboxyl groups. The literature reposted that Sago *hampas* consists of 64.4% cellulose, 25.1% hemicelluloses, and 10.5% lignin. Lignocellulosic bands will be retained in several strong absorption bands in the regions of 800–500 cm^{-1}, 1200–1000 cm^{-1}, and 1620–1600 cm^{-1} [24].

The common glycosidic linkages explain that the presence of the absorption band at 1020 cm^{-1}, 1029 cm^{-1}, 1114 cm^{-1}, 1149 cm^{-1}, 1236 cm^{-1}, and 1244 cm^{-1} was attributed to C-O-C ring vibrational stretching of β for cellulose I and cellulose II; it was suggested that the characteristics of hemicelluloses are more prominent in Sago hampas [24].

The absorption band at 1519 cm^{-1} with smaller peak was exhibited as C=C stretching vibrations of the aromatic rings of lignin. However, it is too weak to be identified as a peak and this was suggested as the low lignin content [24].

3.4. Sago Composite with Different Particle Size Analysis by DSC. The DSC thermograms of Sago particleboard with different particle size are shown in Figure 9. The DSC was performed to check the moisture content and volatile component present in samples. The result shows that as the temperature increased on the particleboard, the chemical activity was able to be identified based on the DSC analysis and proved that moisture content and volatile components have great effect on the properties of particleboard [6].

Based on the result, all the endotherm peak is within temperature range at about 50°C–200°C. The endotherm peak occurred at 88°C for sample C, 82°C for sample B, and 76°C for sample A. Sample C showed higher amount of water molecules in the sample compared with samples A and B;

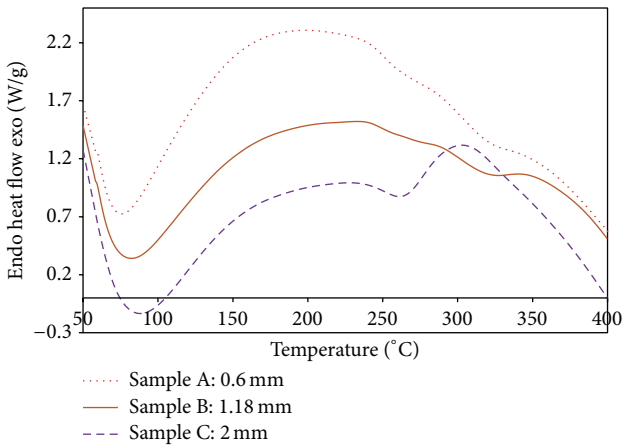

Figure 9: Sago/UF Sample with different size of particle analysis by DSC.

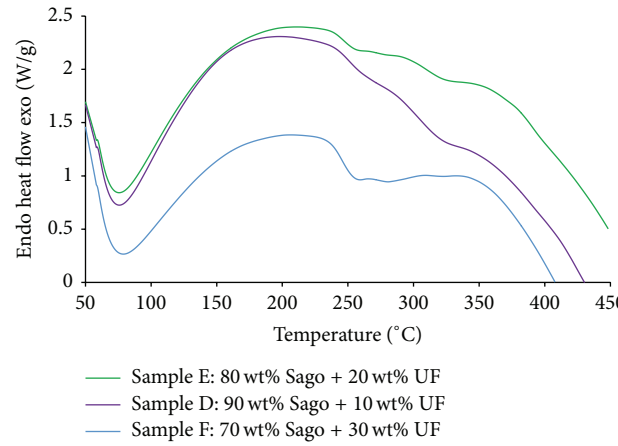

Figure 10: Sago/UF Sample with different weight fraction analysis by DSC.

this was proved by TGA. The small reduction on endotherm peak was observed in both samples A and B. This indicated a smaller amount of water molecules in the samples [6].

The result showed that higher melting temperature occurred on bigger particles. The higher melting temperature was found at 88°C for sample C and the lowest was found at 76°C for sample A. Bigger particles contain more starch compared to smaller particles and will explore more matrix. This is contributed by the cross-linking reaction between the starch granules and leads to better interaction between starch, UF, and the particles in the panel [27]. Hence, this will contribute to higher strength of panel and required more heat to complete the melting process [27].

Generally, decomposition of the natural fibre begins in between 200 and 360°C [6, 18]. Based on the result, sample C showed a single endothermic peak at 263°C due to thermal decomposition of Sago particles. Sample A exhibited two endothermic peaks at 263°C and 322°C; sample B exhibited two endothermic peaks at 262°C and 318°C. The double endothermic peaks obtained in DSC thermograms were due to the thermal decomposition of Sago and Sago filled with UF.

In addition, sample C exhibited a second exotherm peak at 303°C, whereas no second exotherm peak was observed in samples A and B. Sample with single exotherm was found to be more thermally stable than those with multiple exotherm peak.

Based on the result, sample A is loosely packed in the structure order compared to sample C which is denser in packing [7]. Sample A cured more compared to sample C because it did not fully bond with the UF. Therefore, smaller particles are easily explored with UF due to smaller surface area. This caused the smaller particles to have better bonding compared with the bigger particles. Besides, smaller particles that bonded with UF also possess better curing characteristic, thus improving the thermal stability properties of the particle. Covalent bonds can be formed in the composite systems, although the dispersion of particles is an important factor for contributing to the enhanced thermal stability [4]. As the UF becomes cross-linked the residual heat of curing becomes smaller and is causing the sample to cure more [28]. It seems that the particles size plays a synergistic role in improving the thermal resistance of the composite.

3.5. Sago Composite with Different Weight Fraction Analysis by DSC. Figure 10 shows the DSC thermogram of Sago particleboard with different weight fraction. The organic compound had melted and decomposed with the pattern as shown in the thermogram in Figure 10 [28]. This showed that amorphous structure occurred in the particleboard and the liquid crystals remained anisotropic after the melting peak [28]. Sample F reached the melting peak at 80°C, sample E at 78°C, and sample D at 77°C, respectively. The lower temperature peak is caused by the structural reorganization and amorphous portion that developed into crystallinity [29].

Based on the result, sample E showed better curing properties than sample D. This is due to the sufficiency of UF applied on Sago particles, which had created homogeneous dispersion in the particleboard and improved the cross-linking reaction between the starch granules [27].

The largest area of sample F showed the least curing properties compared to other samples and requested maximum of heat release due to the Sago particles and UF curing and water reaction [30]. This could be due to excessive matrix where there is little change of the crystal perfection or degree of crystallinity by increasing the weight fraction during manufacturing process [29]. Hence, the curing period becomes longer. The increase in the melting temperature can be attributed by two factors: incomplete curing reaction and increase in the free volume of the system [8]. The decrease in the free volume is proposed to be responsible for increasing the melting temperature because of the addition of matrix in the particleboard. On the other hand, the particleboard with different loadings of Sago particles and matrix had higher melting temperature which may be attributed to the reinforcement effect and restrict the motion between Sago particles and matrix that leads to increase in T_m [4].

Sample F had the compact packing in structure order while sample E of the particleboard had looser packing in

Table 1: Results for Sago/UF Sample with different particle size analysis by TGA.

Size	Temperature range (°C)	Temperature peak (°C)	Weight loss (%)	Residue (%)
Sample A	62–161	75	3	27
0.6 mm	184–539	312	71	
Sample B	55–168	82	2	25
1.18 mm	176–574	311	73	
Sample C	55–175	86	9	15
2 mm	193–585	311	76	

the structure order which required smaller amount of heat to achieve curing and melting.

By comparing the crystallization between samples D and F, sample F showed exothermic peak with lower temperature of 201°C compared to sample D which was 208°C. This is due to additional Sago particles that shifted the exothermic peak toward the higher temperature and the nucleating of the Sago particles in the crystallization of UF matrix [30]. Sago particles acted as heterogeneous nucleation agents for UF.

Sample F showed a single endothermic peak between 200°C and 350°C due to thermal decomposition of Sago particles. The samples are reduced to fibres and char in an inert atmosphere [29]. Samples D and E exhibited multiendothermic peak due to thermal decomposition of Sago particles and filled polymer UF in the Sago particles [6]. This was shown on the basis of prominent changes occurring in the structure and the chemical reaction with secondary reaction [6, 28].

3.6. Sago Composite with Different Particle Size Analysis by TGA. The thermal behaviour of Sago particleboard with different particles size was determined. Figure 11 and Table 1 show the details of the decomposition of the Sago particles. It can be seen that sample C has the highest weight loss at the beginning, which is about 9%. This is attributed to the higher moisture content trapped in the particleboard. The moisture evaporated from the particles starting earlier than other samples around 55°C–175°C with longer time and higher temperature [4]. Sample C has bigger surface area to trap more moisture compared to smaller size particles. This is because the presence of hemicelluloses has caused higher moisture absorption of the composite [4].

Besides, the bigger size of particles did not fully bond with the matrix and had created voids between the particles, hence reducing the strength of the particleboard. The addition of surface area caused reduction in the thermal stability of composite due to the influence of less stable particles [4]. The OH groups in Sago particles attracted water molecule through hydrogen bonding, thus making it dimensionally unstable, which had caused physical, mechanical, and chemical properties changes [6].

Sample A had better thermal stability compared to sample C. This is because reducing the size can help the particles to bond well with UF and improve the decomposing process [31]. Smaller size of particles allows covalent bonds to form easily in the composite systems. The dispersion of particles in the particleboard is also an important factor that contributes

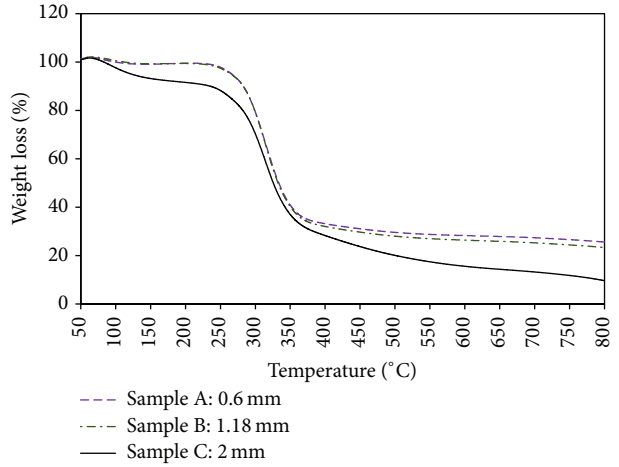

Figure 11: Sago/UF Sample with different size of particle analysis by TGA.

to the enhancement of thermal stability [7]. Besides, smaller particles have best surface-to-volume ratio and this caused decomposition temperature to be greater than the larger particle size. The smaller the particle size, the greater the extent equilibrium temperature [7]. Sample A has lower percentage of weight loss initially due to small area of surface trapping small amount of moisture.

3.7. Sago Composite with Different Weight Fraction Analysis by TGA. Thermal stability is one of the most important parameters of UF/Sago particleboard to determine their suitability in actual applications. The thermal stability of particleboards by using different weight fractions of matrix is shown in Figure 12 and the details of decomposition were shown in Table 2. It shows that different matrix loading in particleboard will lead to different thermal stability level. All the specimens were decomposed in a single stage of decomposition. The first step is associated with the moisture loss or the evaporation of trapped solvent. The second step is associated with the weight loss process corresponding to dehydration reaction on polymer chain which usually occurred from 180°C to 570°C. The final step is associated with the residues at 450°C in order to produce the carbon.

Sample D decomposed more after three steps, that is, 3% of mass loss in the first step, 71% of mass loss in second step,

Table 2: Results for Sago/UF Sample with different weight fraction analysis by TGA.

Weight fraction (wt%)	Temperature range (°C)	Temperature peak (°C)	Mass loss (%)	Residue (%)
Sample D	62–161	75	3	27
	184–539	312	71	
Sample E	60–136	74	2	41
	207–534	308	58	
Sample F	55–167	76	3	27
	183–569	306	71	

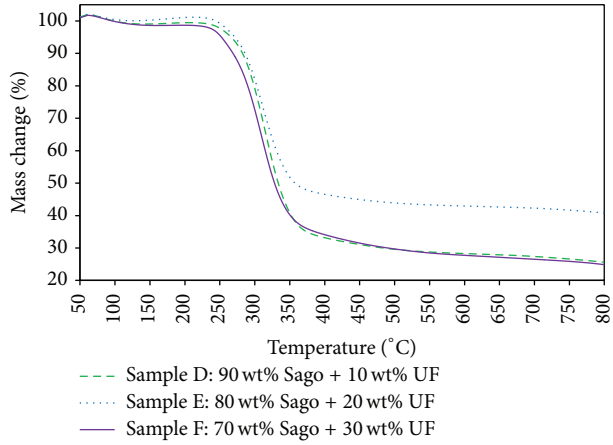

Figure 12: Sago/UF Sample with different weight fraction analysis by TGA.

and 27% of mass loss in the last step. The peak degradation temperature is 312°C.

There are three thermogravimetric regions that appeared on sample E. In the first region (60°C–136°C) there was a small peak due to loss of water absorption. In the second region (207°C–534°C), formation of volatile combustible compounds and high loss of weight took place. In the third thermogravimetric region, it belonged to residue and formation of char. Based on the TGA curve, the decomposition rate was around 305°C to 312°C. According to the thermal behaviour of the UF/Sago particleboard, hot pressing temperature at 160°C is suitable for the UF and Sago to react without thermal decomposition [32].

Sample F with 3% of mass loss is observed from 55°C to 167°C followed by the major weight loss of 71% at the second stage. Then, at the final stage, the residues are found to be 27%.

The pyrolysis of UF/Sago particleboard took place below 250°C. Researcher has mentioned that pyrolysis of hemicellulose, lignin, and cellulose usually occurred at 200°C, 220°C, and 250°C, respectively, with carbon dioxide and water [6, 32]. Sample E with 20 wt% of UF matrix has strong interaction between Sago particles in the composites. UF matrix acts as a cross-linker that reacts with the cell wall hydroxyl group of Sago and creates a rigid linking bridge with Sago particles. Hence, the thermal stability of Sago particle is enhanced [6].

Sample E is more thermally stable because the weight loss percentage is low during the degradation process compared to other specimens. However, sample D with 10 wt% of matrix and sample F with 30 wt% of matrix did not show good thermal stability properties. This is because 10 wt% is not sufficient for particles bonding while the 30 wt% is excessive for particle bonding. By introducing 20 wt% matrix into the particleboard, better thermal stability can be attained due to the proper characteristic structure in a polymer matrix as well as their shape and dimension of particles being close to each other. Hence, 20 wt% matrix can lead to better bonding between the matrix and particles [32]. The strong interaction between particles and polymer matrix has caused the motions of polymer chains to be limited and increased the stabilization in the UF/Sago particleboard [32]. Excessive matrix had evaporated during the hot press process and will reduce the strength for the whole specimen. 20 wt% of matrix can increase the resistance of particleboards to thermal degradation, alter their pyrolysis route, and increase the amount of char produced [33]. The strength of the composite will be reduced by the presence of numerous hydroxyl groups (-OH) in the Sago components. The OH groups in Sago attract water molecule through hydrogen bonding, thus causing it to be dimensionally unstable and properties changed in terms of physical, mechanical, and chemical properties [6].

Sample E has the lowest percentage of weight loss at the first stage due to the composite being trapped by small amount of water. This has caused the Sago particles to have better bonding between each other without hydroxyl groups.

The different observations in these three particleboard are probably due to the different weight fraction used to manufacture the boards which indicates that the weight fraction is significant to thermal stability behaviour.

4. Conclusions

The analysis of particleboard through IB, Screw Test, TGA, FTIR, and DSC showed little difference between each other by changing of weight fraction and size of particles. The boards' strength is enhanced when the resin loading is increased, but this is only applicable to certain percentage of resin loading and after that the strength will drop and over matrix will increase the manufacturing cost. The results from TGA showed that the addition of Sago fibre into the Sago/UF composite slightly improved both the charring capability and thermal stability. From the TGA/DSC study, it can be concluded that sample with 20 wt% matrix and particles size 0.6 mm sample had better thermal stability and better curing

properties. This is because the samples were fully bonded by the UF matrix. Based on the TGA, the degradation of hemicellulose, cellulose, and lignin can be observed followed by a further slow degradation until a fixed carbon was achieved at 800°C. FTIR analysis showed the concurrences of bonding between functional groups of Sago fibre and UF, which confirmed that the reactions between all the components have been taking place in the composite system. All the particleboards that met the M-0, M-1, M-2, and M-3 specification of American National Standard A208.1-2009 fulfilled the industrial and commercial application.

Conflict of Interests

The authors declare that there is no conflict of interests regarding the publication of this paper.

Acknowledgments

The authors would like to acknowledge the Faculty of Engineering at Universiti Malaysia Sarawak, Hexzachem Sarawak Sdn Bhd, and The Forestry Sarawak for the use of their lab facilities and support.

References

[1] D. S. Awg-Adeni, S. Abd-Aziz, K. Bujang, and M. A. Hassan, "Bioconversion of sago residue into value added products," *African Journal of Biotechnology*, vol. 9, no. 14, pp. 2016–2021, 2010.

[2] P. A. P. Mamza, E. C. Ezeh, E. C. Gimba, and D. E. Arthur, "Comparative study of phenol formaldehyde and urea formaldehyde particleboards from wood waste for sustainable environment," *International Journal of Scientific & Technology Research*, vol. 3, no. 9, pp. 53–61, 2014.

[3] S. Oza, R. Wang, and N. Lu, "Thermal and mechanical properties of recycled high density polyethylene/hemp fiber composites," *International Journal of Applied Science and Technology*, vol. 1, no. 5, pp. 31–36, 2011.

[4] V. Chandra Sekhar, V. Pandurangadu, and T. Subba Rao, "TGA, DSC, DTG properties of epoxy composites reinforced with feather fibers of 'Emu' bird," *International Journal of Innovative Research in Science, Engineering and Technology*, vol. 3, no. 5, pp. 13017–13023, 2014.

[5] S.-Y. Fu, X.-Q. Feng, B. Lauke, and Y.-W. Mai, "Effects of particle size, particle/matrix interface adhesion and particle loading on mechanical properties of particulate-polymer composites," *Composites Part B: Engineering*, vol. 39, no. 6, pp. 933–961, 2008.

[6] M. S. Islam, S. Hamdan, H. R. Sobuz, R. Rahman, and A. S. Ahmed, "Thermal and decay-resistance properties of tropical wood-plastic composites," *Journal of Composite Materials*, vol. 47, no. 12, pp. 1493–1500, 2012.

[7] T. Hatakeyama and F. X. Quinn, *Thermal Analysis—Fundamentals and Applications to Polymer Science*, John Wiley & Sons, 1994.

[8] Z. N. Azwa and B. F. Yousif, "Thermal degradation study of kenaf fibre/epoxy composites using thermos gravimetric analysis," in *Proceedings of the 3rd Malaysian Postgraduate Conference (MPC '13)*, pp. 256–264, Sydney, Australia, July 2013.

[9] T. C. Chiang, S. Hamdan, and M. S. B. Osman, "The effect of weight fraction and size on the properties of sago particles urea formaldehyde particleboard," *Jurnal Teknologi*, vol. 73, no. 1, pp. 61–67, 2015.

[10] JIS A 5908, *Japanese Industrial Standard Particle Boards*, Japanese Standards Association, 1994.

[11] M. Jani and I. Kamal, "Mechanical and physical properties of low density kenaf core particleboards bonded with different resins," *Journal of Science and Technology*, vol. 4, no. 1, 2012.

[12] Z. Pan, Y. Zheng, R. Zhang, and B. M. Jenkins, "Physical properties of thin particleboard made from saline eucalyptus," *Industrial Crops and Products*, vol. 26, no. 2, pp. 185–194, 2007.

[13] S. M. Jani, M. P. Koh, M. Suffian, M. Rafeadah, and R. Salmiah, "Development of low density particleboard using kenaf core: mechanical and physical testing results," *Journal of Science and Technology*, 2010.

[14] M. Jawaid, H. P. S. Abdul Khalil, and A. Abu Bakar, "Hybrid composites of oil palm empty fruit bunches/woven jute fiber: chemical resistance, physical, and impact properties," *Journal of Composite Materials*, vol. 45, no. 24, pp. 2515–2522, 2011.

[15] R. O. Ebewele, B. H. River, and G. E. Myers, "Behavior of amine-modified urea-formaldehyde-bonded wood joints at low formaldehyde/urea molar ratios," *Journal of Applied Polymer Science*, vol. 52, no. 5, pp. 689–700, 1994.

[16] Z. Cai, Q. Wu, J. N. Lee, and S. Hiziroglu, "Influence of board density, mat construction, and chip type on performance of particleboard made from eastern redcedar," *Forest Products Journal*, vol. 54, no. 12, pp. 226–232, 2004.

[17] V. Vassiliou and I. Barboutis, "Screw withdrawal capacity used in the eccentric joints of cabinet furniture connectors in particleboard and MDF," *Journal of Wood Science*, vol. 51, no. 6, pp. 572–576, 2005.

[18] A. J. H. Ahmad, J. Kasim, and A. L. Mohmod, "Properties of single-layer urea formaldehyde particleboard manufactured from commonly utilized malaysian bamboo (*Gigantochloa scortechinii*)," *Journal of Bamboo and Rattan*, vol. 1, no. 2, pp. 109–117, 2002.

[19] M. E. Selamat, O. Sulaiman, R. Hashim et al., "Measurement of some particleboard properties bonded with modified carboxymethyl starch of oil palm trunk," *Measurement*, vol. 53, pp. 251–259, 2014.

[20] J. Zhang, X. Wang, S. Zhang, Q. Gao, and J. Li, "Effects of melamine addition stage on the performance and curing behavior of melamine-urea-formaldehyde (MUF) resin," *BioResources*, vol. 8, no. 4, pp. 5500–5514, 2013.

[21] A. Gurses, S. Karagoz, F. Mindivan, K. Gunes, C. Dogar, and S. Akturk, "Preparation and characterization of urea/formaldehyde/rosa *Canina* sp. seeds composites," in *Proceedings of the 3rd International Advances in Applied Physics and Materials Science Congress (APMAS '13)*, vol. 125, Antalya, Turkey, April 2013.

[22] N. Sarifuddin, H. Ismail, and Z. Ahmad, "The effect of kenaf core fibre loading on properties of low density polyethylene/thermoplastic sago starch/kenaf core fiber composites," *Journal of Physical Science*, vol. 24, no. 2, pp. 97–115, 2013.

[23] B. Yaacob, M. C. I. M. Amin, K. Hashim, and B. A. Bakar, "Optimization of reaction conditions for carboxymethylated sago starch," *Iranian Polymer Journal*, vol. 20, no. 3, pp. 195–204, 2011.

[24] S. F. Sim, M. Mohamed, N. A. L. M. I. Lu, N. S. P. Sarman, and S. N. S. Samsudin, "Computer-assisted analysis of fourier thransform infrared (FTIR) spectra for characterization of various treated and untreated agriculture biomas," *Bioresources*, vol. 7, no. 4, pp. 5367–5380, 2012.

[25] Z. Ahmad, H. Anuar, and Y. Yusof, "The study of biodegradable thermoplastics sago starch," *Key Engineering Materials*, vol. 471-472, pp. 397–402, 2011.

[26] M. S. Islam, S. Hamdan, and M. R. Rahman, "Effects of polymer loading on tropical wood polymer composite (WPC)," *Advanced Materials Research*, vol. 264-265, pp. 631–635, 2011.

[27] N. S. Sulaiman, R. Hashim, M. H. M. Amini, O. Sulaiman, and S. Hiziroglu, "Evaluation of the properties of particleboard made using oil palm starch modified with epichlorohydrin," *BioResources*, vol. 8, no. 1, pp. 283–301, 2013.

[28] UserCom 1/2000, Chapter 11: Information for users of Mettler Toledo thermal analysis systems, http://www.masontechnology.ie/x/Usercom_11.pdf.

[29] D. D. L. Chung, "Thermal analysis of carbon fiber polymer-matrix composites by electrical resistance measurement," *Thermochimica Acta*, vol. 364, no. 1-2, pp. 121–132, 2000.

[30] H. Bouafif, A. Koubaa, P. Perré, A. Cloutier, and B. Riedl, "Wood particle/high-density polyethylene composites: thermal sensitivity and nucleating ability of wood particles," *Journal of Applied Polymer Science*, vol. 113, no. 1, pp. 593–600, 2009.

[31] T. W. Goodrich, *The physical properties and microstructural changes of composite materials at elevated temperature [Master of Science in Mechanical Engineering]*, 2009.

[32] C. E. Corcione and M. Frigione, "Characterization of nanocomposites by thermal analysis," *Materials*, vol. 5, no. 12, pp. 2960–2980, 2012.

[33] P. S. Karastergiou and J. L. Philippou, "Thermogravimetric analysis of fire retardant treated particleboard," in *Wood and Fire Safetry*, pp. 385–394, 2000.


Journal of
Nanotechnology

International Journal of
Corrosion

International Journal of
Polymer Science

Smart Materials
Research

Journal of
Composites

BioMed
Research International
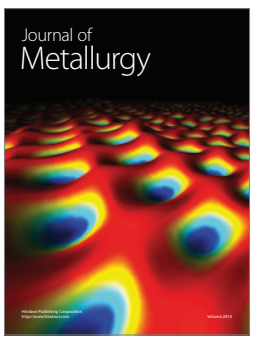
Journal of
Metallurgy

Journal of
Materials

Hindawi
Submit your manuscripts at
http://www.hindawi.com
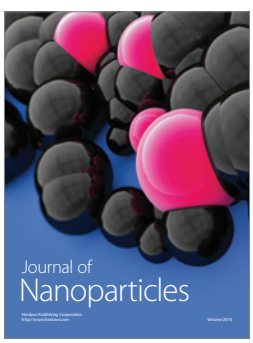
Journal of
Nanoparticles
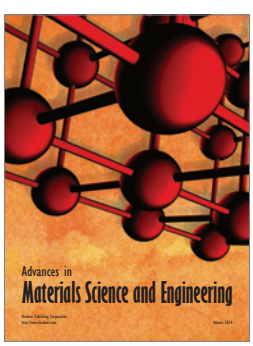
Advances in
Materials Science and Engineering
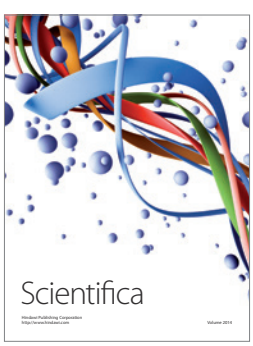
Scientifica
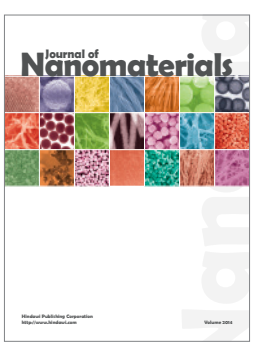
Journal of
Nanomaterials

The Scientific
World Journal

International Journal of
Biomaterials
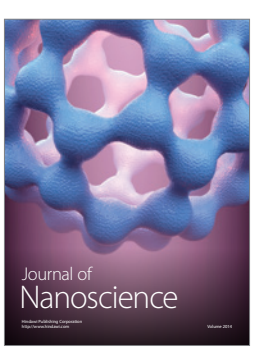
Journal of
Nanoscience

Journal of
Coatings
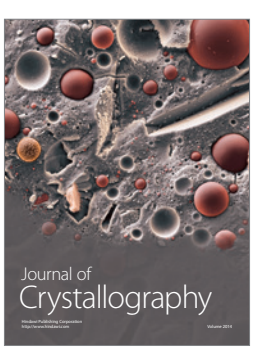
Journal of
Crystallography

Journal of
Ceramics
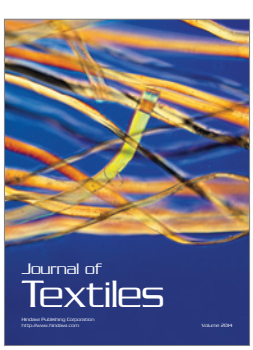
Journal of
Textiles